Electronic Supplementary Material (ESI) for Journal of Materials Chemistry C.

Supporting information

New cyclopentadithiophene (CDT) linked porphyrin donors with different end capping acceptors for efficient small molecule organic solar cells

Susana Arrechea,[a,b] Ana Aljarilla,[a] Pilar de la Cruz,[a] Emilio Palomares,[c,d] Manish Kumar Singh[e], Ganesh D. Sharma,[e*] Fernando Langa.[a*]

[a]Universidad de Castilla-La Mancha. Institute of Nanoscience, Nanotechnology and Molecular Materials (INAMOL), Campus de la Fábrica de Armas, Toledo. Spain. Tel: 34 9252 68843. *E-mail: Fernando.Langa@uclm.es

[b]Escuela de Ingeniería Química, Facultad de Ingeniería, Universidad de San Carlos de Guatemala, Ciudad Universitaria, 11 Av., Guatemala 01012, Guatemala. E-mail: arrecheausac@gmail.com

[c]Institute of Chemical Research of Catalonia (ICIQ). Avda. Països Catalans, 14. Tarragona. E-43007. Spain. E-mail: epalomares@iciq.es

[d]ICREA. Passeig Lluis Companys, 23. Barcelona. E-08010. Spain.

[e]Department of Physics, The LNM Institute of Information Technology (Deemed University), Rupa ki Nagal, Jamdoli, Jaipur (Raj.) 302031, India. *E-mail: gdharma273@gmail.com

1. Materials and methods

Synthetic procedures were performed under Argon atmosphere, in dry solvent unless otherwise noted. All reagents and solvents were reagent grade and were used without further purification. Chromatographic purifications were performed using silica gel 60 SDS (particle size 0.040-0.063 mm). Analytical thin-layer chromatography was performed using Merck TLC silica gel 60 F254. ^{1}H NMR spectra were obtained on Bruker TopSpin AV-400 (400 MHz) spectrometer. Chemical shifts are reported in parts per million (ppm) relative to the solvent residual peak ($CDCl_3$, 7.27 ppm). ^{13}C NMR chemical shifts (δ) are reported relative to the solvent residual peak ($CDCl_3$, 77.0 ppm). Fourier transform infrared spectrophotometer (FT-IR) Thermo Nicolet AVATAR 370 was used. UV-Vis measurements were carried out on a Shimadzu UV 3600 spectrophotometer. For extinction coefficient determination, solutions of different concentration were prepared in CH_2Cl_2 (HPLC grade) with absorption between 0.1-1 of absorbance using a 1 cm UV cuvette. The emission measurements were carried out on Cary Eclipse fluorescence spectrophotometer. Mass spectra (MALDI-TOF) were recorded on a VOYAGER DE™ STR mass spectrometer using dithranol as matrix. Melting points are uncorrected.

The molecular geometries and frontier molecular orbitals of these new dyes have been optimized by density functional theory (DFT) calculations at the B3LYP/6-31G* level using Gaussian09W.[S1] Cyclic voltammetry was performed in ODCB-acetonitrile (4:1) solutions. Tetrabutylammonium perchlorate (0.1 M as supporting electrolyte) were purchased from Acros and used without purification. Solutions were deoxygenated by argon bubbling prior to each experiment, which was run under argon atmosphere. Experiments were done in a one-compartment cell equipped with a platinum working microelectrode (∅ =

S1. Gaussian 09, Revision E.01, M. J. Frisch, G. W. Trucks, H. B. Schlegel, G. E. Scuseria, M. A. Robb, J. R. Cheeseman, G. Scalmani, V. Barone, B. Mennucci, G. A. Petersson, H. Nakatsuji, M. Caricato, X. Li, H. P. Hratchian, A. F. Izmaylov, J. Bloino, G. Zheng, J. L. Sonnenberg, M. Hada, M. Ehara, K. Toyota, R. Fukuda, J. Hasegawa, M. Ishida, T. Nakajima, Y. Honda, O. Kitao, H. Nakai, T. Vreven, J. A. Montgomery, Jr., J. E. Peralta, F. Ogliaro, M. Bearpark, J. J. Heyd, E. Brothers, K. N. Kudin, V. N. Staroverov, R. Kobayashi, J. Normand, K. Raghavachari, A. Rendell, J. C. Burant, S. S. Iyengar, J. Tomasi, M. Cossi, N. Rega, J. M. Millam, M. Klene, J. E. Knox, J. B. Cross, V. Bakken, C. Adamo, J. Jaramillo, R. Gomperts, R. E. Stratmann, O. Yazyev, A. J. Austin, R. Cammi, C. Pomelli, J. W. Ochterski, R. L. Martin, K. Morokuma, V. G. Zakrzewski, G. A. Voth, P. Salvador, J. J. Dannenberg, S. Dapprich, A. D. Daniels, Ö. Farkas, J. B. Foresman, J. V. Ortiz, J. Cioslowski, and D. J. Fox, Gaussian, Inc., Wallingford CT, 2009.

2 mm) and a platinum wire counter electrode. An $Ag/AgNO_3$ (0.01 M in CH_3CN) electrode was used as reference and checked against the ferrocene/ferrocenium couple (Fc/Fc^+) before and after each experiment.

The thermal stability was evaluated by TGA on a Mettler Toledo TGA/DSC Starte System under nitrogen, with a heating rate of 10 ºC/min. Heating of crystalline samples leads to melting of the solids, but no recrystallization was observed.

2. ^{1}H NMR, ^{13}C NMR, FT-IR and MALDI-TOF MS spectra

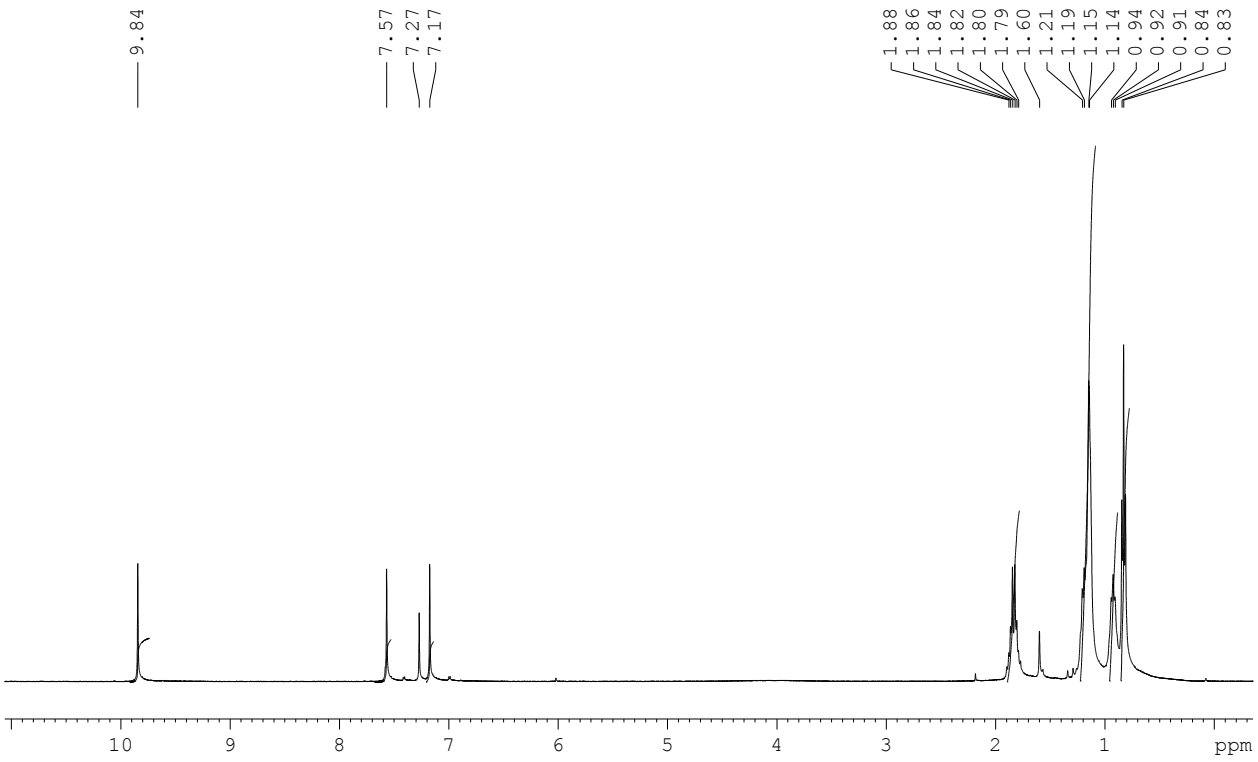

Figure S1. ^{1}H NMR spectrum (400 MHz, $CDCl_3$) of **2**.

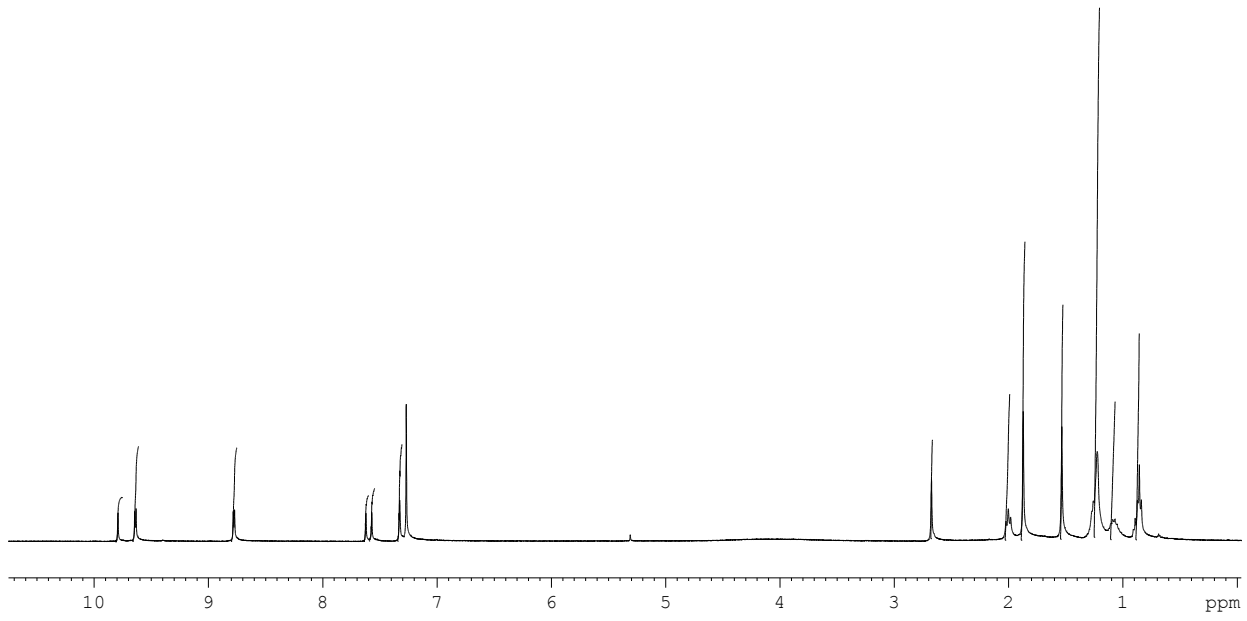

Figure S2. ^{1}H NMR spectrum (400 MHz, $CDCl_3$) of **4**.

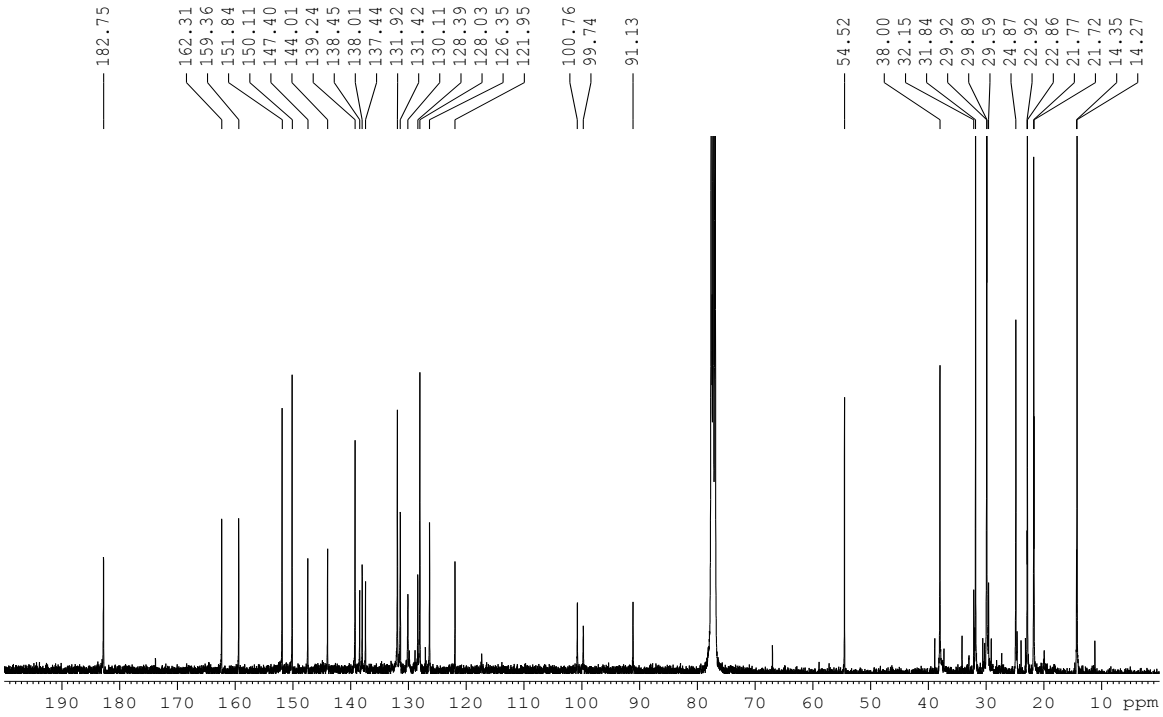

Figure S3. ^{13}C NMR spectrum (100 MHz, $CDCl_3$) of **4**.

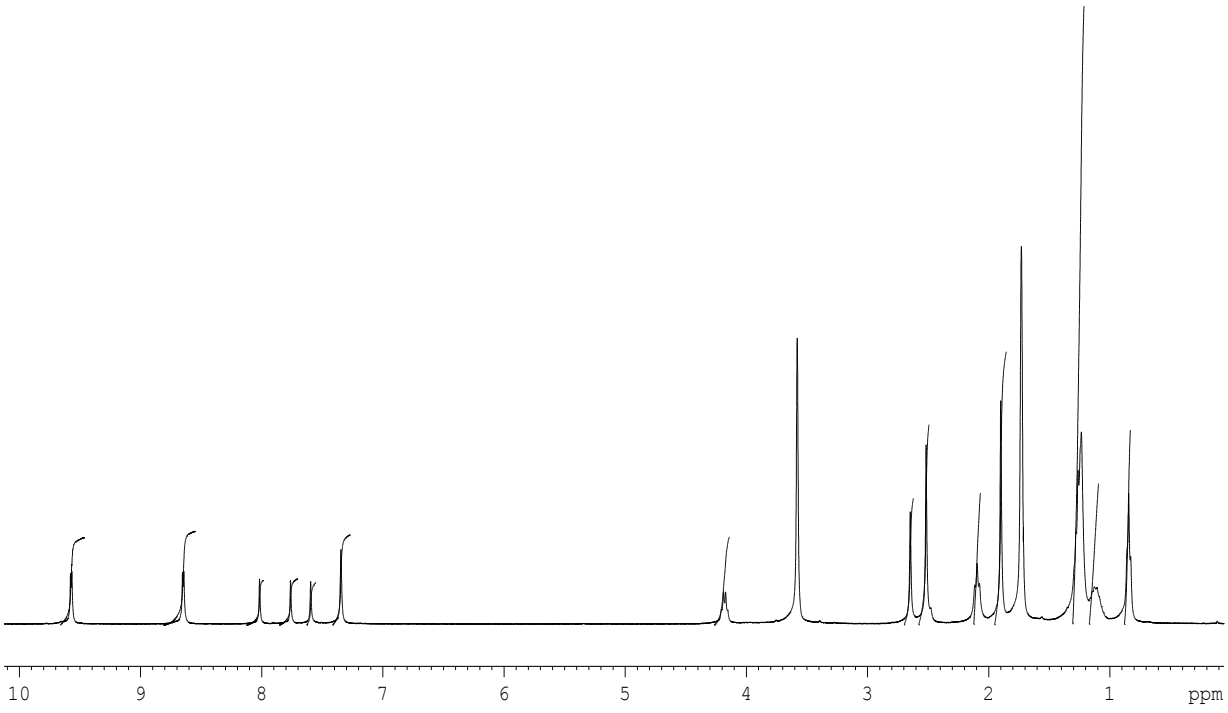

Figure S4. ^{1}H NMR spectrum (400 MHz, $CDCl_3$) of **SA1**.

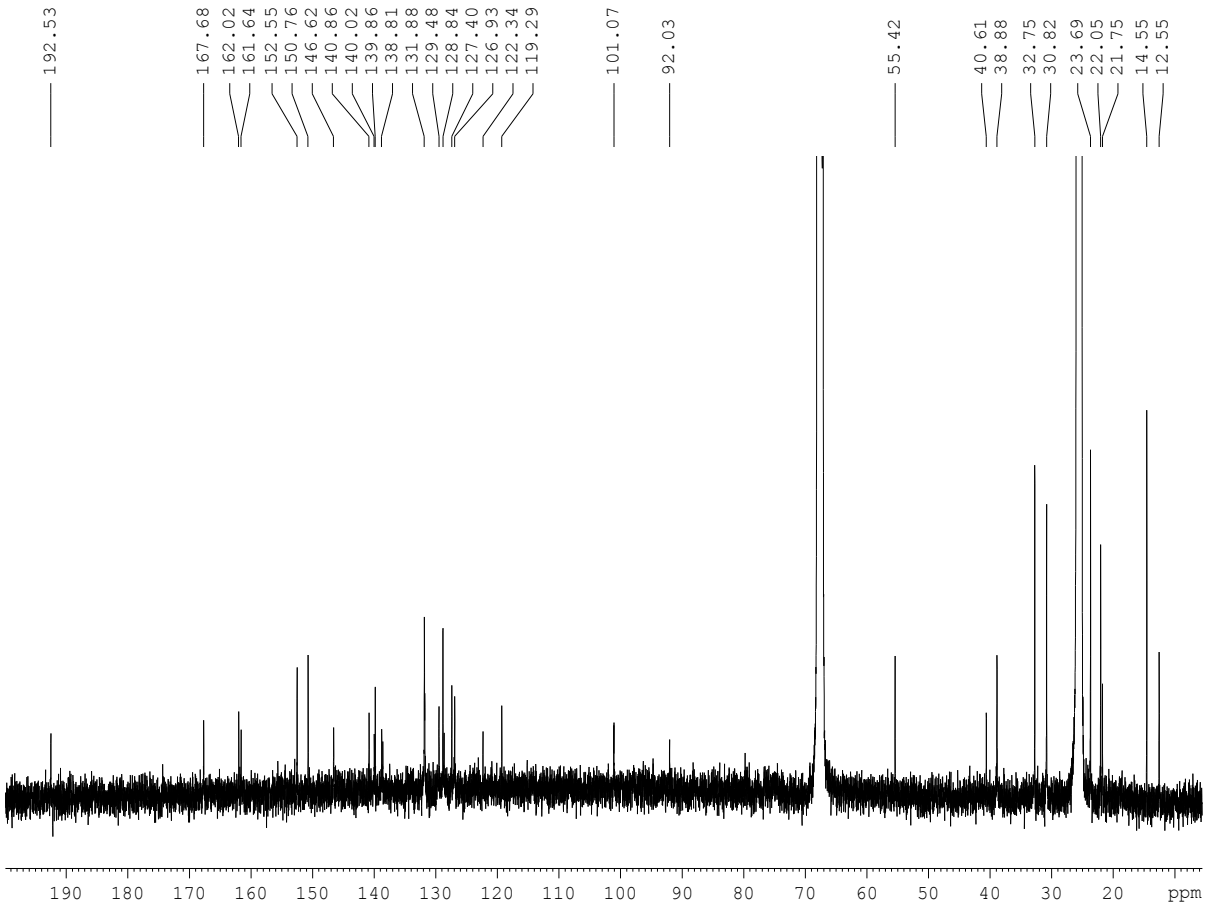

Figure S5. ^{13}C NMR spectrum (100 MHz, $CDCl_3$) of **SA1**.

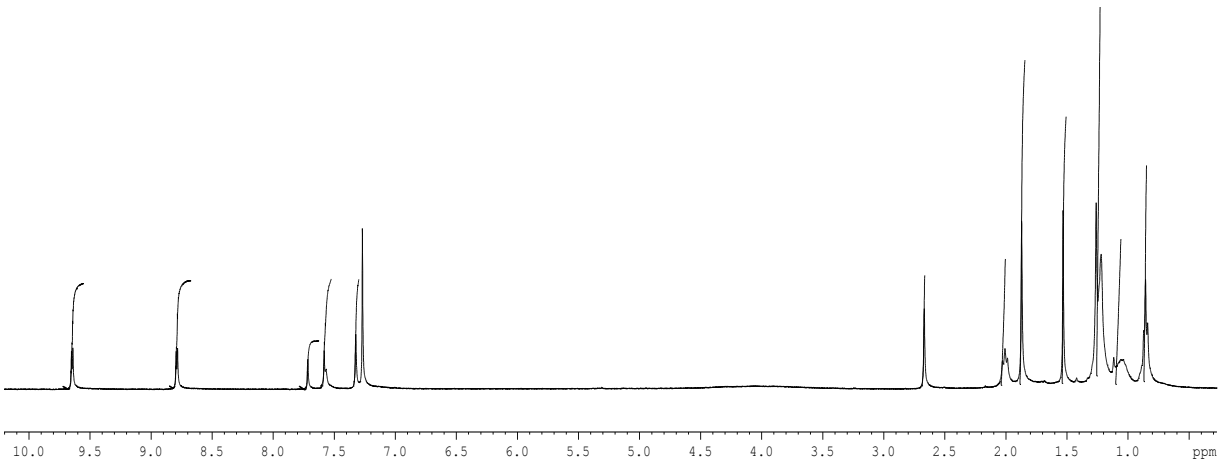

Figure S6. ^{1}H NMR spectrum (400 MHz, $CDCl_3$) of **SA2**.

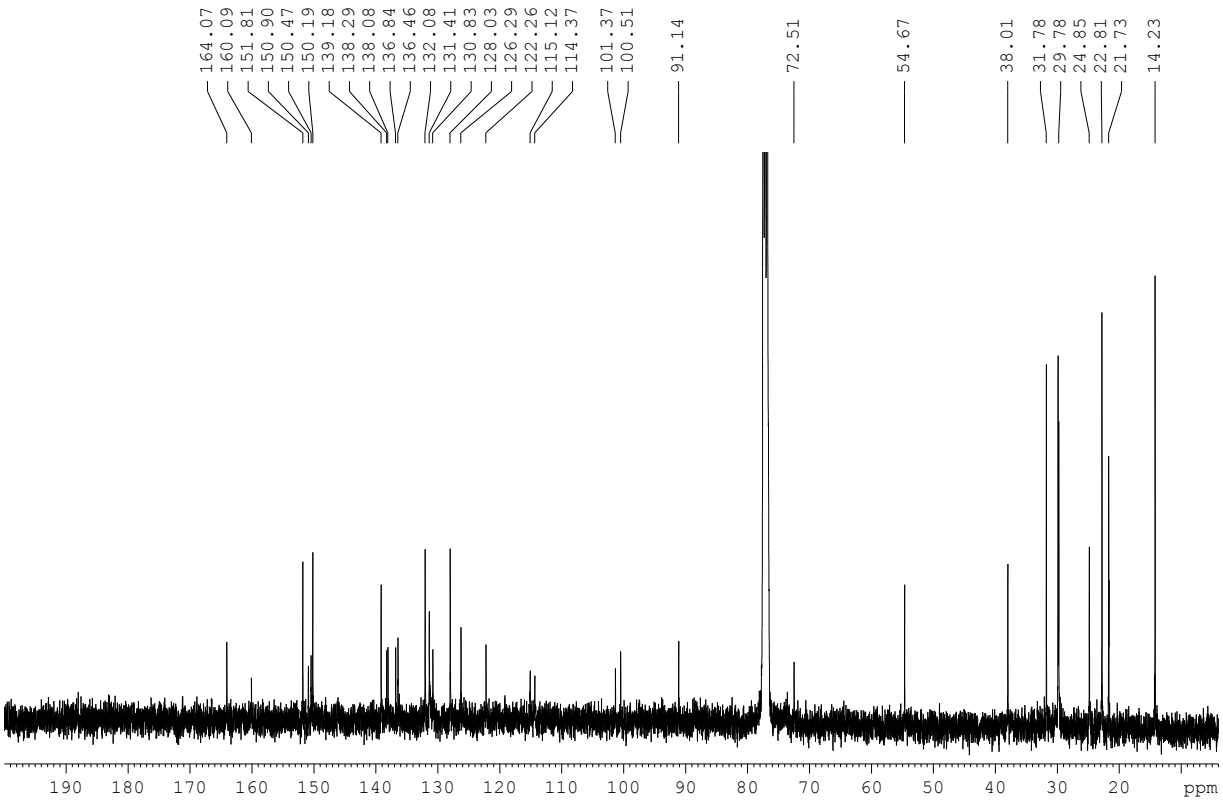

Figure S7. ^{13}C NMR spectrum (100 MHz, $CDCl_3$) of **SA2**.

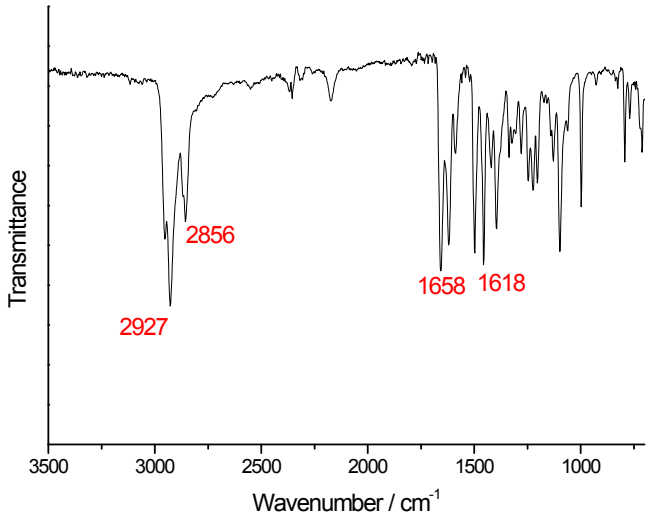

Figure S8. FT-IR spectrum of compound **4** (NaCl window)

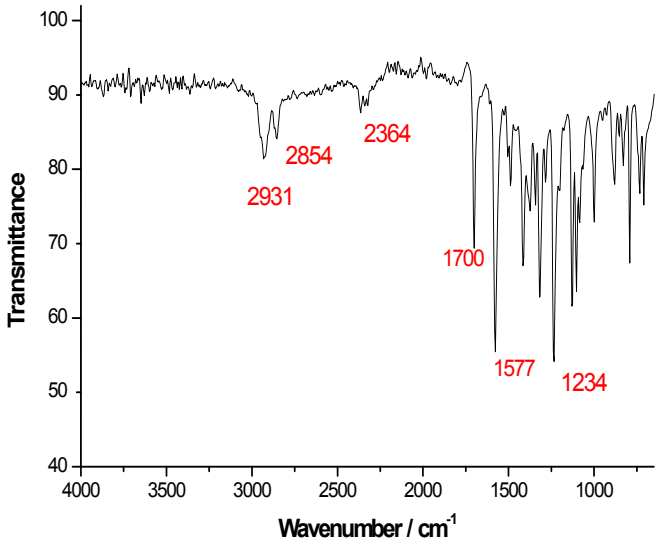

Figure S9. FT-IR spectrum of compound **SA1** (NaCl window).

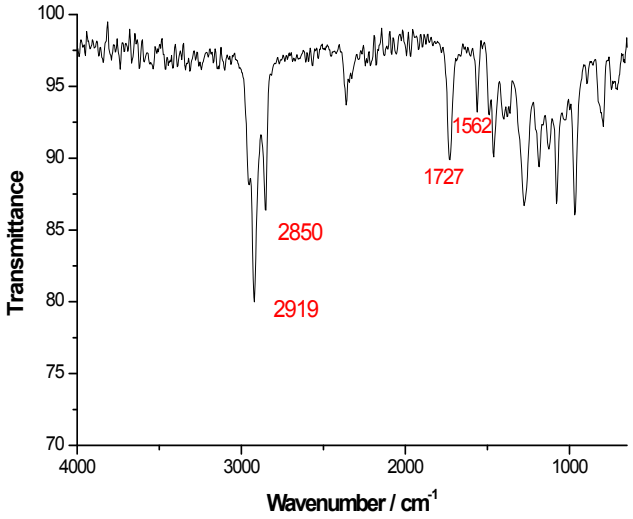

Figure S10. FT-IR spectrum of **SA2** (NaCl window).

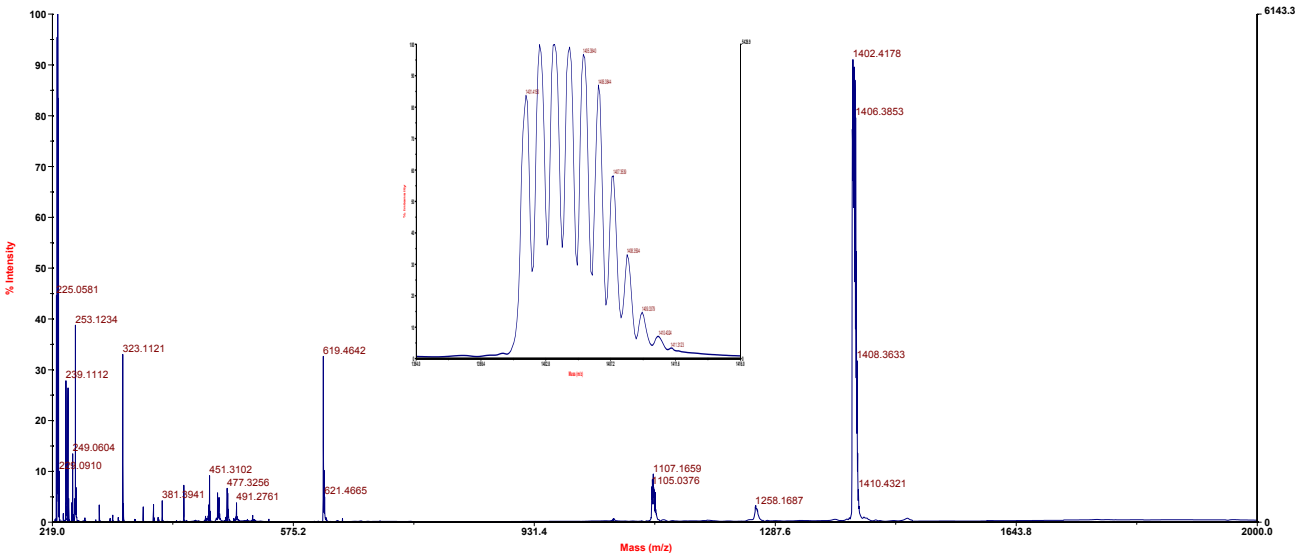

Figure S11. MALDI-TOF MS spectrum of compound **4** (Matrix: Dithranol).

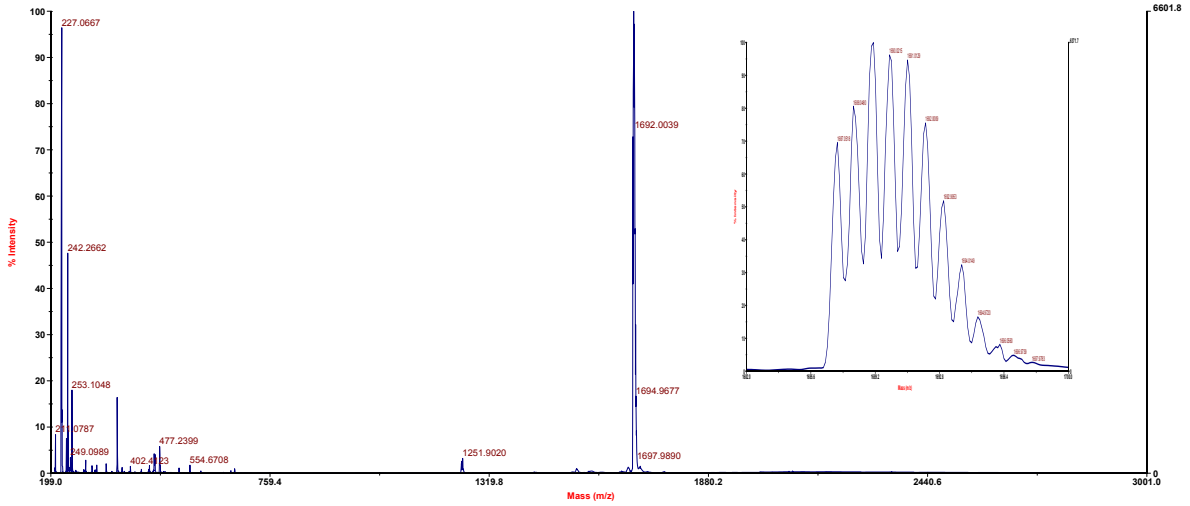

Figure S12. MALDI-TOF MS spectrum of compound **SA1** (Matrix: Dithranol).

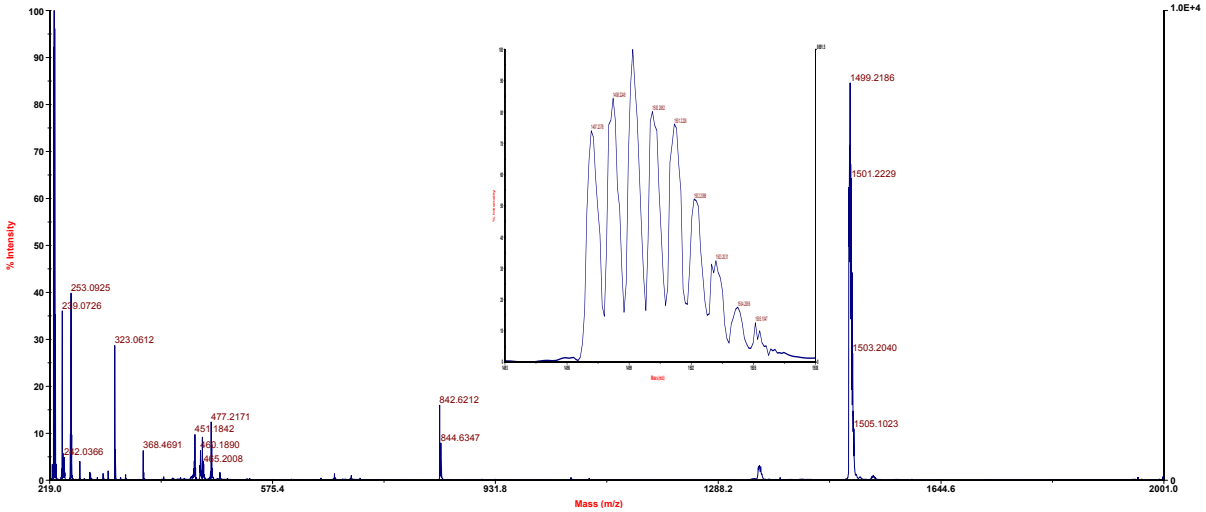

Figure S13. MALDI-TOF MS spectrum of compound **SA2** (Matrix: Dithranol).

3. Thermogravimetric analysis of compounds SA1 and SA2.

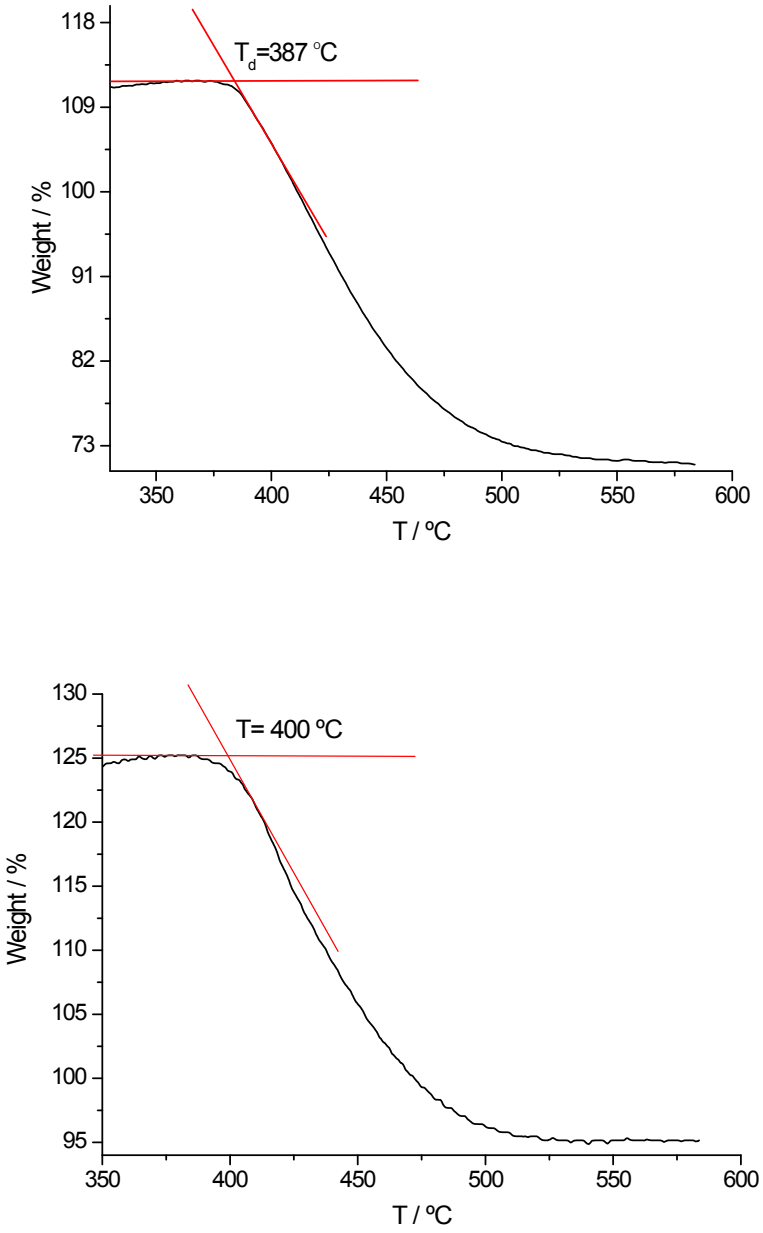

Figure S14. Thermogravimetric analysis of **SA1** (up) and **SA2** (down).

4. Electrochemical studies

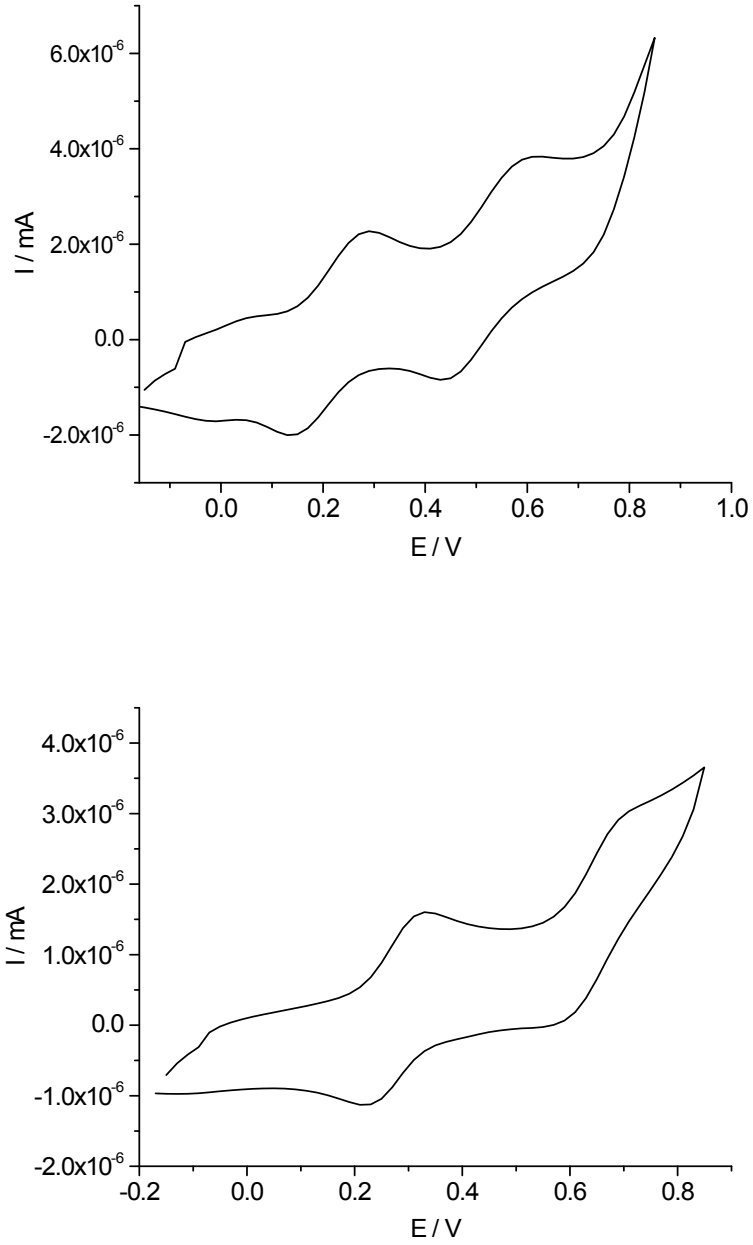

Figure S15. Cyclic voltammetries (anodic window) of **SA1** (up) and **SA2** (down) (referred to Fc/Fc^{+}).

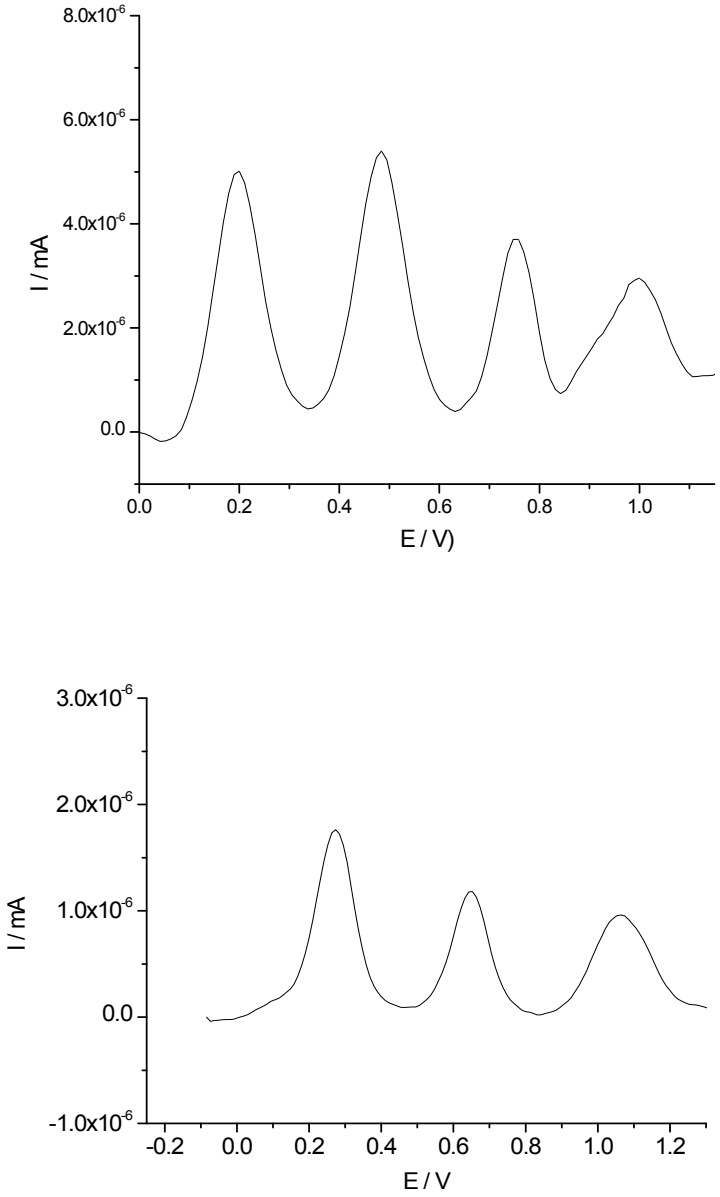

Figure S16. OSWV voltammetries (anodic window) of **SA1** (up) and **SA2** (down) (referred to Fc/Fc^{+}).

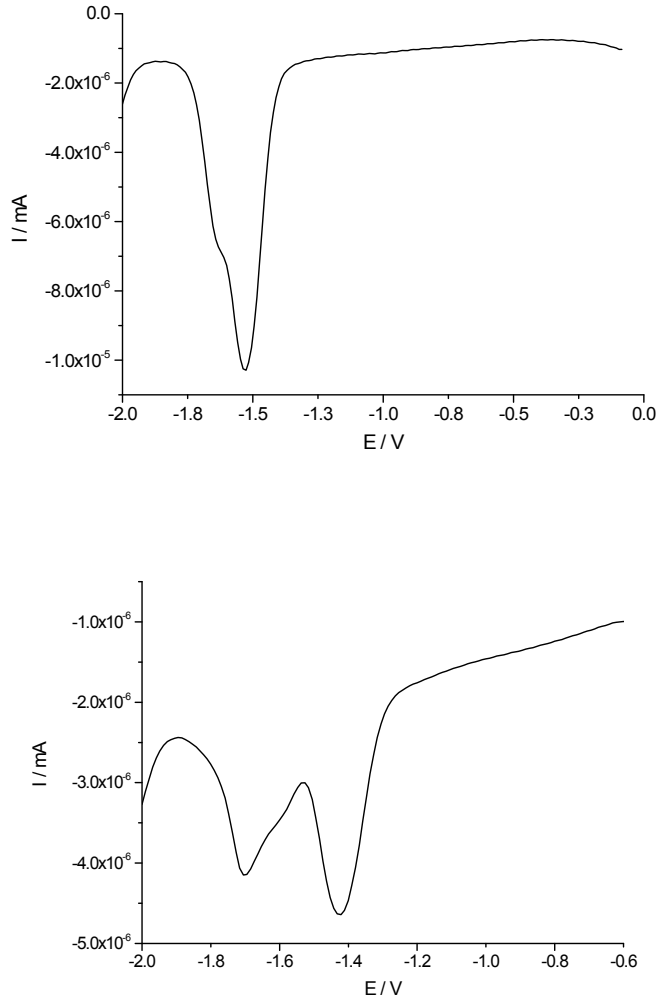

Figure S17. OSWV voltammetries (cathodic window) of **SA1** and **SA2** (referred to Fc/Fc^{+}).

5. Theoretical Calculations.

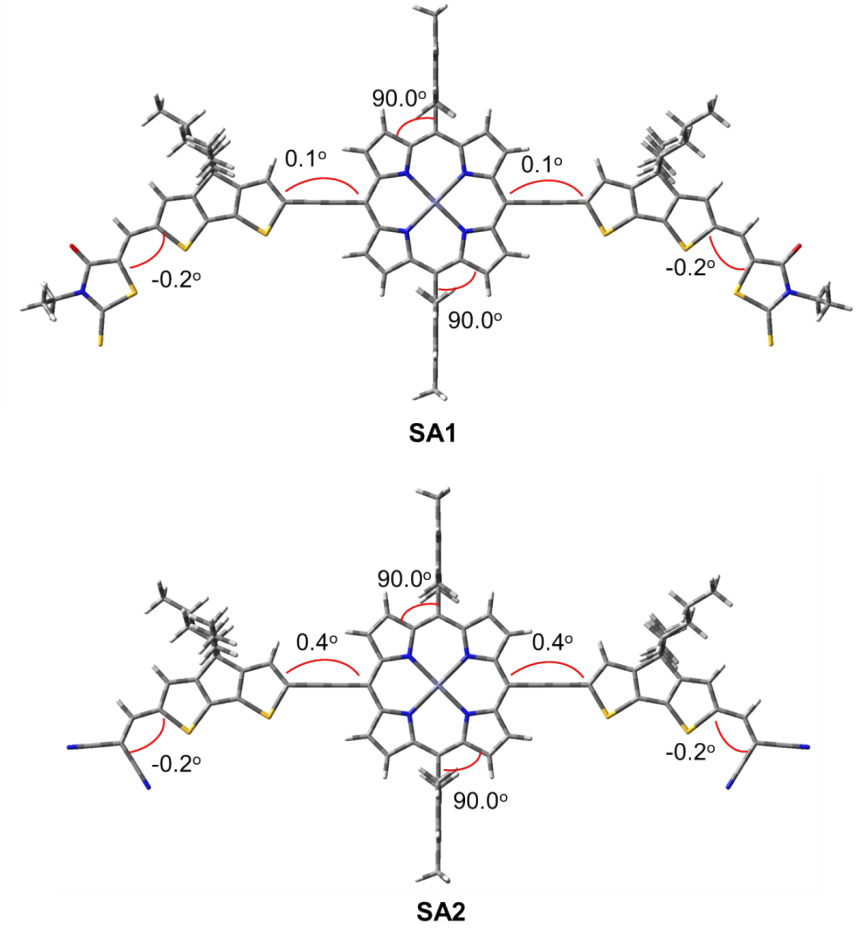

Figure S18. Theoretical optimized geometries and dihedral angles of **SA1** and **SA2**.

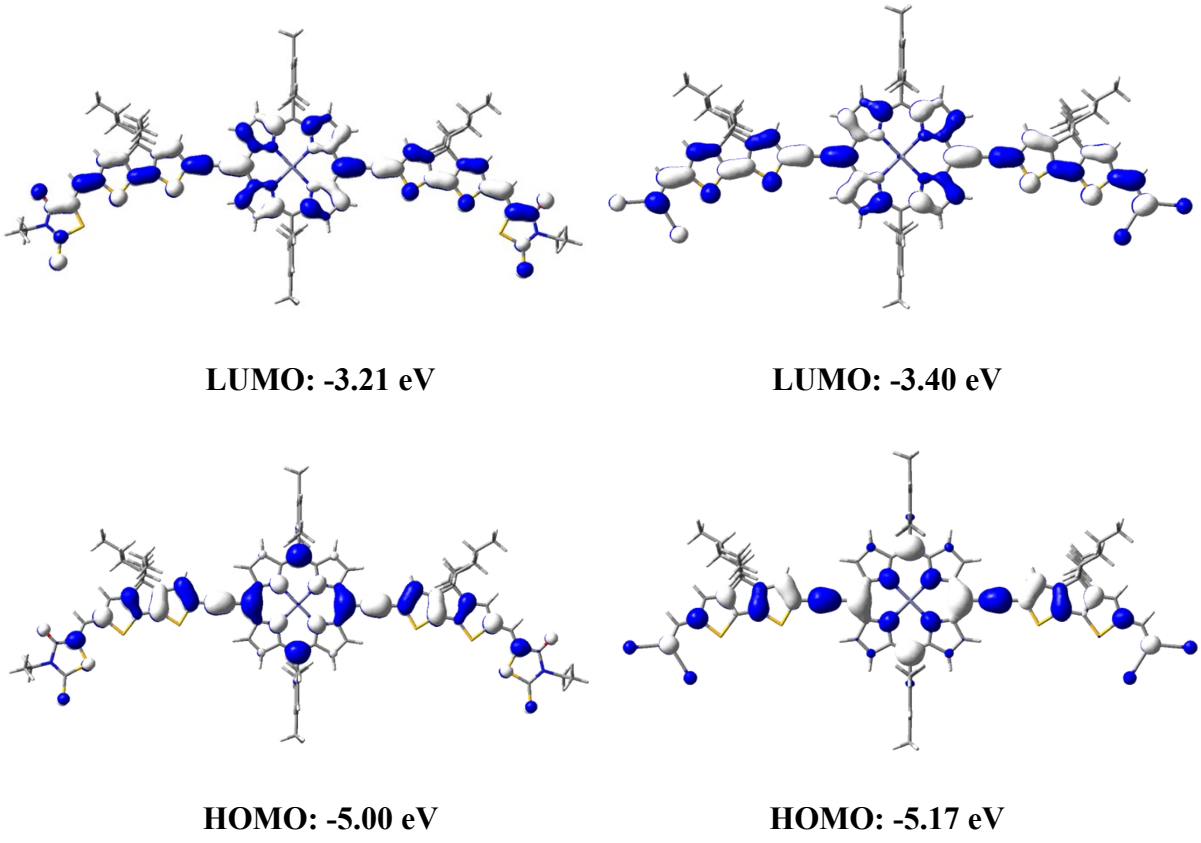

Figure S19. Electronic density contours and energy levels for HOMO and LUMO calculated for **SA1** (left) and **SA2** (right).

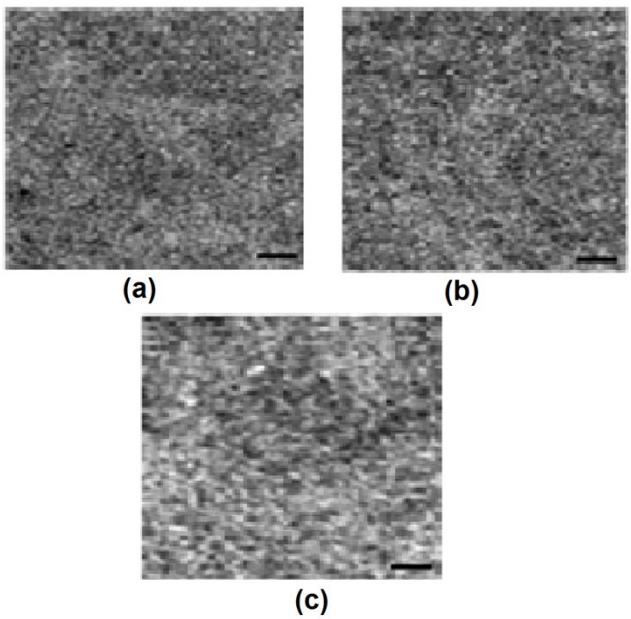

Figure S20. TEM images of the **SA2:**PC71BM processed with (a) CB, (b) DIO/CB and (c) DIO/CB/SVA. Bar scale is 100 nm.

Table S1 Photovoltaic parameters of CB cast S**A1**:$PC_{71}BM$ (different weight ratios) based organic solar cells

SA1 to $PC_{71}BM$ weight ratios	J_{sc} (mA/cm^2)	V_{oc} (V)	FF	PCE (%)
1:05	4.32	0.88	0.32	1.22
1:1	5.16	0.89	0.34	1.56
1:1.5	6.84	0.90	0.38	2.34
1:2	7.61	0.90	0.40	2.73
1.2.5	7.36	0.89	0.36	2.36

Table S2 Photovoltaic parameters of CB cast S**A2**:$PC_{71}BM$ (different weight ratios) based organic solar cells

SA2 to $PC_{71}BM$ weight ratios	J_{sc} (mA/cm^2)	V_{oc} (V)	FF	PCE (%)
1:05	5.31	0.96	0.35	1.78
1:1	6.82	0.98	0.37	2.47
1:1.5	7.85	0.96	0.40	3.01
1:2	8.56	0.98	0.42	3.52
1.2.5	8.06	0.98	0.39	3.08

Table S3 Photovoltaic parameters of DIO/CB cast (different volume concentration of DIO) S**A1**:$PC_{71}BM$ (1:2) based organic solar cells

DIO (v%) concentration	J_{sc} (mA/cm^2)	V_{oc} (V)	FF	PCE (%)
1	8.33	0.88	0.49	3.59
2	9.54	0.89	0.51	4.33
3	12.46	0.85	0.55	5.82
3.5	11.86	0.83	0.52	5.12

Table S4 Photovoltaic parameters of DIO/CB cast (different volume concentration of DIO) S**A2**:$PC_{71}BM$ (1:2) based organic solar cells

DIO (v%) concentration	J_{sc} (mA/cm^2)	V_{oc} (V)	FF	PCE (%)
1	9.27	0.89	0.49	4.04
2	10.98	0.91	0.54	5.39
3	13.12	0.91	0.57	6.80
3.5	12.68	0.89	0.55	6.21